Available online at www.sciencedirect.com
ScienceDirect
Journal of Power Sources 168 (2007) 346–350
JOURNAL OF POWER SOURCES
www.elsevier.com/locate/jpowsour

Short communication

On the activity and stability of Sr_3NiPtO_6 and Sr_3CuPtO_6 as electrocatalysts for the oxygen reduction reaction in a polymer electrolyte fuel cell

Per Kjellin [a,*], Henrik Ekström [b], Göran Lindbergh [b], Anders E.C. Palmqvist [a,c]

[a] *Applied Surface Chemistry, Department of Chemical and Biological Engineering, Chalmers University of Technology, SE-412 96 Göteborg, Sweden*
[b] *Department of Applied Electrochemistry, Royal Institute of Technology (KTH), Stockholm, Sweden*
[c] *Competence Centre for Catalysis, Chalmers University of Technology, SE-412 96 Göteborg, Sweden*

Received 28 November 2006; received in revised form 23 February 2007; accepted 24 February 2007
Available online 2 March 2007

Abstract

Sr_3NiPtO_6 and Sr_3CuPtO_6 were evaluated as low-platinum alternative oxygen reduction catalysts in a solid polymer electrolyte fuel cell at 80 °C. The oxides were synthesised using a new method based on an organometallic precursor route. The electrochemical evaluation showed similar oxygen reduction performance for Sr_3NiPtO_6 and Sr_3CuPtO_6, with a slightly higher activity for Sr_3NiPtO_6. In comparison with the oxides, the oxygen reduction activity for a commercial Pt/C catalyst was approximately 10 times higher. XRD analysis of the used electrodes revealed that the oxides were not stable in the PEMFC environment, and converted into platinum during operation. Elemental analysis of the used electrodes also showed a difference in platinum formation, where the platinum content on the surface of the electrode facing the gas diffusion layer was several times higher for Sr_3NiPtO_6 than Sr_3CuPtO_6. This indicates that the Sr_3NiPtO_6 electrode may be more susceptible to platinum migration.

Keywords: Platinum oxide; Sr_3NiPtO_6; Sr_3CuPtO_6; Fuel cell; PEMFC

1. Introduction

The polymer electrolyte fuel cell technology still has some obstacles to overcome before broad commercialisation will be possible. As long as the operating temperature of the polymer electrolyte is limited to below 100 °C a relatively large amount of platinum or platinum alloys has to be used in order to catalyse the electrode reactions. In a hydrogen–oxygen (or air) polymer fuel cell the platinum needed in the cathode is especially high, due to the relatively sluggish oxygen reduction reaction (ORR). Hence, the platinum used in the electrodes is likely to make up a significant cost of the fuel cell system.

From a cost perspective there is thus a great need to decrease the platinum content of the ORR catalyst material. Alternative methods studied to achieve this include using the platinum more efficiently, for example by decreasing the size of the platinum particles [1], or by using platinum alloys or oxides with a lower platinum content. Platinum alloys, such as Pt–Co have shown to be very efficient [2–4], but suffer from stability problems [5,6]. There are also a few studies of ORR catalysts which do not contain any platinum, for example Fe(II) deposited on carbon [7,8].

Besides the lower platinum content in mixed platinum oxides, they may be more stable than alloys and thus an attractive alternative to platinum. In direct methanol fuel cells (DMFC) where platinum is used there is an additional problem with a lowered cathode potential due to fuel permeation through the polymer membrane [9,10], and platinum oxides may be less susceptible to such methanol poisoning.

Oxoplatinates with the 2-H perovskite structure, such as Sr_3NiPtO_6, have previously been shown to possess a remarkably high ORR activity [11], and would thus be a promising candidate as a cathode catalyst. In the present study, a new synthesis method for Sr_3NiPtO_6 and the related Sr_3CuPtO_6 was developed to allow for a higher specific surface area of the metal oxides, and with the aim of further improving the ORR performance of these catalysts. Fuel cell electrodes were made using the synthesized catalysts, and a series of fuel cell experiments were conducted in different gas atmospheres with the objective to evaluate the oxygen reduction and hydrogen oxidation activ-

* Corresponding author. Tel.: +46 31 772 29 72.
E-mail address: per.kjellin@promimic.se (P. Kjellin).

0378-7753/$ – see front matter © 2007 Elsevier B.V. All rights reserved.
doi:10.1016/j.jpowsour.2007.02.051

ity. Also, the electrochemically active surface was investigated using cyclic voltammetry in inert (nitrogen) atmosphere. The results were compared to a commercial Pt/C catalyst. Finally, the stability of the catalysts was evaluated through structural and elemental characterization of the electrode, both prior to and after the fuel cell experiments.

2. Experimental

2.1. Synthesis of materials

In a typical experiment, stoichiometric amounts, 0.642 g of platinum acetylacetonate (Pt-acac, 48.0% Pt, Alfa Aesar), 0.419 g Ni-acac (95%, Aldrich) and 1.40 g Sr-acac (97%, Aldrich) were mixed with 5 mL of diethylene glycol (99%, Aldrich). The mixture was heated to 80 °C and kept at this temperature for 4 h under extensive stirring in order to allow the organometallic precursors to dissolve. The resulting gel-like substance was then put in an oven for 6 h at 250 °C in order to evaporate the diethylene glycol. The remaining black powder was placed in a tube furnace, heated to 1100 °C with a heating rate of 2.77 °C min^{-1}, and kept at 1100 °C in air for 3 days. Sr_3NiPtO_6 had a light brown colour, while Sr_3CuPtO_6 was dark brown. To prepare the electrode material, 0.5 g of the product was thoroughly ground in a mortar with 5 mL of 2-propanol (99.5%, Aldrich) and 0.5 g of Vulcan XC-72 carbon (Cabot). Finally, the mixture was put in an oven at 80 °C for 12 h in order to evaporate the 2-propanol. The catalyst powders thus obtained were subsequently used in the preparation of the electrode inks described below. As a reference sample to benchmark the activity a commercial 20% Pt on Vulcan XC-72 from ETEK was used.

Powder XRD measurements were done with a Siemens D5000 diffractometer using Cu Kα radiation (λ = 1.54 Å). EDX analyses were done with a LEO Ultra 55 SEM, equipped with a Oxford Inca EDX system. The error margin for the EDX measurements was less than 2%. Nitrogen adsorption measurements were done with a Micromeritics Tri Star instrument using the BET algorithm to calculate the specific surface area.

2.2. Electrocatalytic testing of catalysts

Nafion 115 membranes from DuPont were successively boiled in 3% hydrogen peroxide, 0.1 M H_2SO_4, and three times in MilliQ water. The membranes were subsequently dried in an oven at 70 °C for 1 h.

Electrode inks were prepared by mixing the catalyst powder with 2% Nafion solution (prepared by diluting 5% Nafion solution from DuPont with equal amounts of MilliQ water and iso-propanol). The ink was rigorously stirred and sonicated for approximately 1 h. Working electrodes were prepared by pipetting 20 μL of the ink onto Nafion 115 membranes placed on a 95 °C hot bed. The electrodes were then left to dry for 15 min on the hot bed. The electrode loading was determined by pipetting the same amount of ink on small pieces of polymer film and measuring the difference in weight before and after pipetting and drying. The Nafion content of all electrodes was 40% by weight. The electrode area was roughly around 0.5 cm^2 with a platinum loading of 0.2 mg cm^{-2}, but varied somewhat between the samples.

The electrode and membrane setup is shown in Fig. 1. Commercial fuel cell MEAs (GORE 5620) were used as combined counter and reference electrodes. One side of the commercial MEA sheet, placed on a 95 °C hot bed, was painted with 50 μL cm^{-2} of 5% Nafion solution using an airbrush and cut into 1.5 cm × 1.5 cm rectangular pieces. Finally, the Nafion painted side of the commercial MEA was hot pressed against the untreated side of the Nafion 115 membranes at 125 °C for 30 s at 1 MPa. It should be noted that only one side of the GORE MEA is operating in the cell. The Nafion painted side is elec-

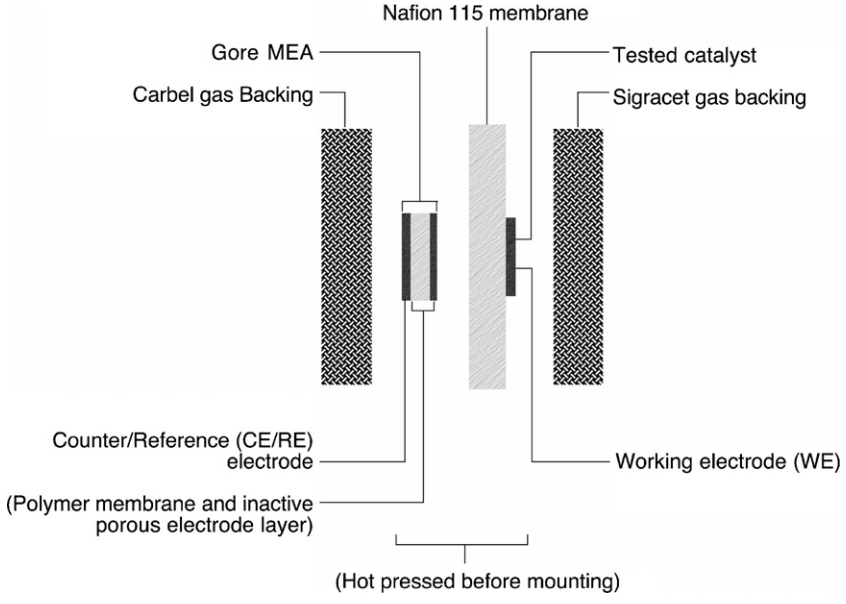

Fig. 1. Electrode and membrane arrangement.

Table 1
Electrochemical measurement protocols describing a potential hold followed by cyclic voltammetry for each gas. Potentials are cell potentials (vs. RHE)

Gases		Measurements	
WE	CE/RE	Potentials	Details
O_2	H_2	Open circuit 1.0 to 0.65 V	30 min 10 mV/s, 10 cycles
N_2	5% H_2 in Ar	0.8 V hold 1.15 to 0.09 V	45 min 100 mV/s, 25 cycles
H_2	H_2	Open circuit −0.2 to 0.2 V	5 min 10 mV/s, 10 cycles

All gases were humidified to 100% relative humidity.

trochemically inactive. The choice of counter electrode was in this case for reproducibility and convenience. In principle any counter electrode with a large platinum area may be used. This double membrane MEA was then mounted in an electrochemical cell described in Ref. [12] with circular 30 mm diameter graphite current collectors with spirally formed gas channels, sandwiched between a Carbel CL gas backing on the counter/reference electrode side and a piece of Sigracet 21 BC gas diffusion media on the working electrode side. The clamping force over current collectors was 400 N.

The fuel cell was connected to a PAR 273A potentiostat, with the pipetted ink electrode as working electrode (WE) and the 0.6 mg Pt cm^{-2} side of the commercial MEA as combined counter and reference electrode (CE/RE). The cell was heated to 80 °C, with gases fed at ambient pressure in excess at 1 mL s^{-1}. All gases were humidified by bubbling the gas through heated humidifiers at 81 °C from Fuel Cell Technologies Inc.

Table 1 shows the electrochemical measurement protocol used for different gases. Several cycles were made for each operating condition in order to get reproducible shapes of the voltammograms, the last cycle was used for evaluation. In general the cell potentials are referred to, but for the cyclic voltammetry measurements in nitrogen the current densities were low, <50 mA cm^{-2}. The CE/RE is not assumed to be polarised during the experiments, and hence these potentials are denoted vs. a relative hydrogen electrode (RHE). Also, these potentials vs. RHE have been corrected for the −45.5 mV Nernstian shift at this temperature due to the lower hydrogen concentration (5% hydrogen in argon). In order to detect any changes in ORR activity due to the changed operating conditions when performing measurements in different gases, a series of measurements on the WE were made in the following order: O_2, N_2, O_2, H_2, N_2, O_2.

3. Results and discussion

3.1. Synthesis of Sr_3NiPtO_6 and Sr_3CuPtO_6

Previous reports on the synthesis of Sr_3NiPtO_6 are based on electrosynthetic flux methods [13,14] or basic alkali melts [15,16]. These methods produce large particulate, low surface area materials which are adequate for single crystal X-ray diffraction but less suitable for catalysis applications. Here, we report a new simple method which gives smaller particles of the oxides.

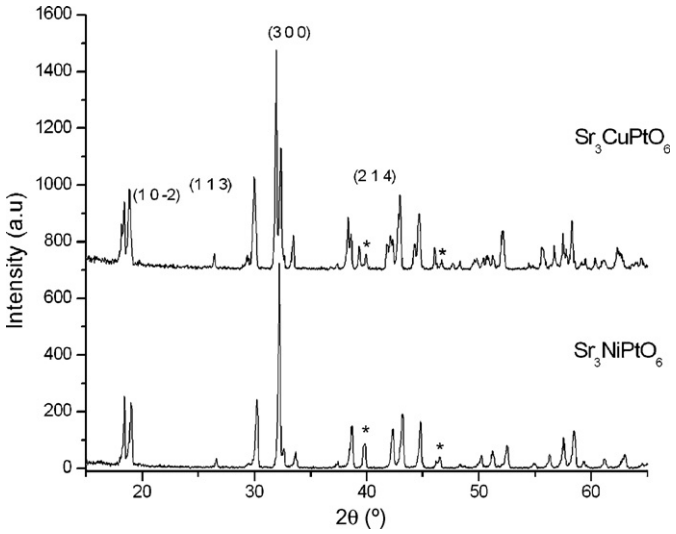

Fig. 2. XRD diffractograms of Sr_3NiPtO_6 and Sr_3CuPtO_6, with indices for the largest peaks shown and (*) showing platinum peaks.

The XRD diffractogram of the as-prepared Sr_3NiPtO_6 and Sr_3CuPtO_6 powders, with a synthesis temperature of 1100 °C, are shown in Fig. 2. The miller indices for the largest peaks are also shown in this figure. There was a very small amount of platinum in both samples, as seen from the platinum peaks at $2\theta = 39.76°$ (1 1 1) and $2\theta = 46.25°$ (2 0 0). The specific surface area for both oxides was 5 m^2/g. Synthesis temperatures below 1100 °C, between 800 and 1050 °C, yielded Sr_3NiPtO_6 or Sr_3CuPtO_6 together with increasing amounts of platinum and Sr_4PtO_6 as the temperature approached 800 °C. For the Sr_3NiPtO_6 synthesis, temperatures below 800 °C produced NiO, Pt and $SrCO_3$. The EDX measurements in Table 2 show that the actual platinum content in the Sr_3CuPtO_6 sample was slightly lower, 7.7 at%, compared to 8.7 at% for the Sr_3NiPtO_6 sample.

3.2. Electrochemical evaluation and stability of Sr_3NiPtO_6 and Sr_3CuPtO_6

In general, the various electrochemical measurements had little impact on the performance of the electrodes made of

Table 2
EDX measurements of Sr_3NiPtO_6 and Sr_3CuPtO_6 powders

Material	Theoretical composition (at%)	EDX measurements (at%)
Sr_3NiPtO_6	27.3 Sr	29.0 Sr
	9.1 Ni	6.7 Ni
	9.1 Pt	8.7 Pt
	54.5 O	55.5 O
Sr_3CuPtO_6	27.3 Sr	27.0 Sr
	9.1 Cu	7.0 Cu
	9.1 Pt	7.7 Pt
	54.5 O	58.3 O

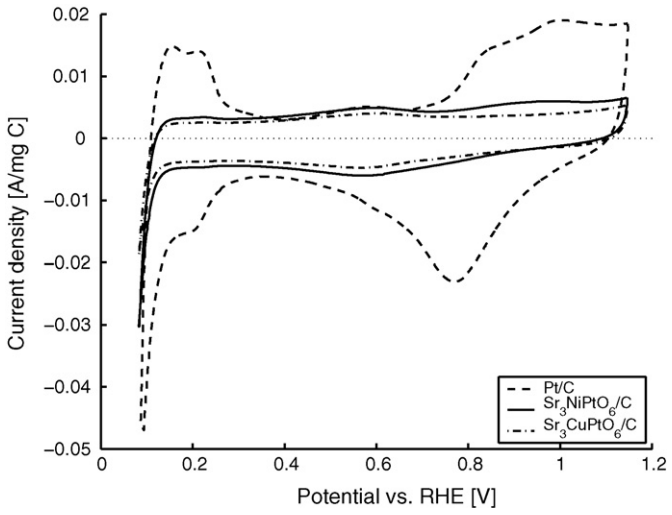

Fig. 3. Cyclic voltammograms in N_2 for Pt/C from ETEK (– – –), Sr_3NiPtO_6/C (—) and Sr_3CuPtO_6/C (– – –). Sweep rate 100 mV s^{-1}, 25th cycle.

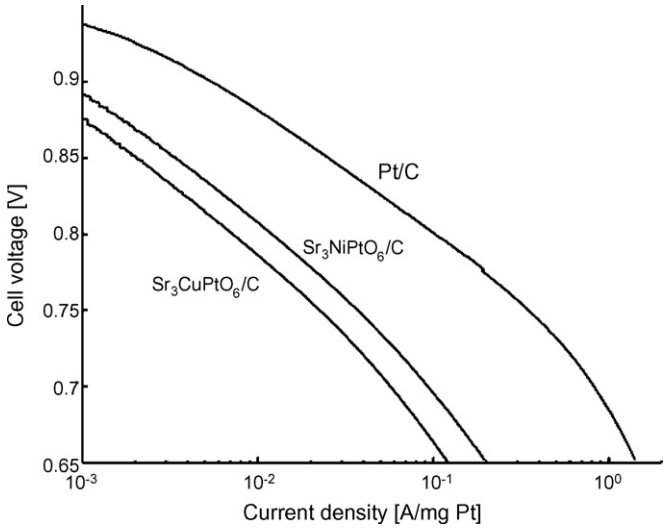

Fig. 4. The mean current vs. potential of the up and down sweep at 10 mV s^{-1} in O_2 for Pt/C from ETEK, Sr_3NiPtO_6/C and Sr_3CuPtO_6/C. IR-corrected, 10th cycle.

ETEK and the oxides; little difference in behaviour could be seen between the first and last measurements in oxygen, or between the two nitrogen runs. For Sr_3CuPtO_6 however, the oxygen reduction activity increased significantly after the first run in N_2, and also somewhat after the H_2 measurement. All measurements described below are from the last runs in nitrogen and oxygen. The hydrogen measurements showed fast hydrogen oxidation kinetics for all electrodes, with a linear dependence of the current on potential, corresponding to an overall cell resistance of around 0.2 Ω cm^2. This measured cell resistance was used for correcting the potentials for ohmic drops in the oxygen measurements.

The cyclic voltammograms in nitrogen (cf Table 1) are shown in Fig. 3. For the ETEK sample, two distinct hydrogen adsorption–desorption ($H_{ads–dsp}$) peaks are seen (0.16 and 0.21 V versus RHE), with an integrated peak area of around 60 C g_{Pt}^{-1} (or 29 m^2 g_{Pt}^{-1}, assuming 210 μC cm_{Pt}^{-2}). Only one peak at a slightly different potential in this region is seen for Sr_3NiPtO_6 (0.24 V versus RHE), and none for Sr_3CuPtO_6. At these low potentials an accurate evaluation of the electrochemically active surface area and active crystal planes of Pt in the Sr_3NiPtO_6 and Sr_3CuPtO_6 electrodes may be difficult since dissolved metal ions from the oxides, for instance presence of Ni^{2+}, are known to affect the shape of cyclic voltammograms of Pt at low potentials due to under potential deposition (UPD) [7], and in addition there are relatively large background currents from the carbon support for the oxide samples. However, a coarse estimate results in roughly 10 times larger peak areas in the low potential region for the ETEK sample compared to the Sr_3NiPtO_6 sample. Also, the shifted peak position for the Sr_3NiPtO_6 sample could be an indication of a different active crystal plane of platinum [17], given that this is not due to UPD effects of Ni.

A similar discrepancy between ETEK and the oxides can be seen in the region between 0.7 and 1.1 V versus RHE, where the magnitude and position of the platinum oxide peaks for Sr_3NiPtO_6 and Sr_3CuPtO_6 have the peak positions shifted, and also have much lower peak areas. Between 0.7 and 1.1 V versus RHE however, metal UPD is less likely to affect the cyclic voltammograms. In all, the cyclic voltammograms in nitrogen indicate electrochemical surfaces similar to carbon supported platinum, with significantly lower active Pt areas for the oxide samples, and possibly a different active crystal plane of platinum for the Sr_3NiPtO_6 sample.

Data from the oxygen reduction measurements, normalized to the same Pt-loading, are shown in Fig. 4. After this, prolonged cycling (1000 cycles) for 20 h in oxygen showed only a minor increase in oxygen reduction for Sr_3NiPtO_6, a slight decrease in activity for ETEK 20%, and no change in activity for Sr_3CuPtO_6. As seen from the figure, the average current density of the Sr_3NiPtO_6 sample is approximately 10% of that of the ETEK sample, i.e. the difference in oxygen reduction activity between ETEK and Sr_3NiPtO_6 is the same as the difference in the assumed platinum surface areas, derived from the cyclic voltammograms in nitrogen.

Table 3 shows the EDX measurements for the oxides and ETEK before and after the fuel cell experiments. After the fuel cell experiments, no strontium, nickel or copper were detected. For both oxides, the platinum content increased somewhat, as a consequence of the decrease in strontium, nickel or copper. But the platinum content in the Sr_3NiPtO_6 sample was considerably higher than in the Sr_3CuPtO_6 sample, 8.5 wt.% compared to 2.4 wt%. The penetration depth for EDX at an acceleration

Table 3
EDX measurements of electrodes before and after fuel cell runs

Electrode	ETEK 20	Sr_3NiPtO_6	Sr_3CuPtO_6
Pt before cell run (wt.%)	13.6	2.5	1.8
Pt after cell run (wt.%)	11.3	8.5	2.4
Sr before cell run (wt.%)	–	5.0	5.0
Sr after cell run (wt.%)	–	0	0
Ni/Cu before cell run (wt.%)	–	0.6	0.8
Ni/Cu after cell run (wt.%)	–	0	0

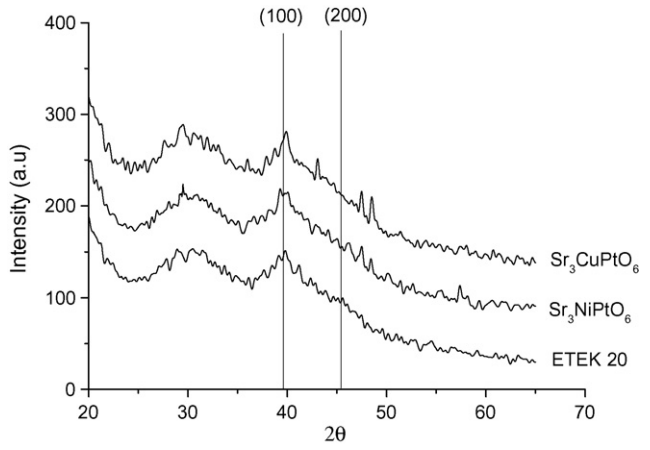

Fig. 5. XRD diffractograms of the electrodes with Sr_3CuPtO_6 (upper graph), Sr_3NiPtO_6 (middle graph), ETEK (lower graph) after the electrochemical measurements. The platinum reflections (1 0 0) and (2 0 0) are shown.

voltage of 15 kV is below 1 μm and the EDX values therefore reflect the atomic content within that depth of the surface of the electrodes which is in contact with the gas diffusion layer. This indicates that Sr_3NiPtO_6 may be more susceptible to platinum migration, a phenomenon which has been reported for Pt/C electrodes [18].

Fig. 5 shows the XRD diffractograms of the materials deposited on the electrodes, after the electrochemical measurements. Apart from the amorphous carbon support which can be seen as a broad peak around $2\theta = 30^\circ$, both samples contain elemental platinum and no trace of the Sr_3MPtO_6 phases is seen. Hence, the measured ORR activity for the oxide electrodes comes from platinum, which is formed during the course of the electrochemical measurements.

4. Conclusions

A new synthesis method for the oxides Sr_3NiPtO_6 and Sr_3CuPtO_6 has been successfully developed, which makes it possible to produce samples with a higher surface area than previously, without the use of alkali flux methods. The electrocatalytic oxygen reduction reaction performance of these two oxides has been investigated in a polymer electrolyte fuel cell environment. The performance of a commercial Pt/C electrode was approximately 10 times higher in comparison. It was found that both oxides degrade in the fuel cell, and were reduced to platinum during the course of the electrochemical evaluation. The degradation and platinum formation mechanism differs between the oxides, for Sr_3NiPtO_6 an enrichment of platinum on the electrode surface facing the gas diffusion layer was observed.

The phenomenon of platinum formation in situ is an interesting one, but from a practical point of view, the use of the oxides as oxygen reduction catalysts in PEM fuel cells is not advisable since the oxides are not sufficiently stable in the fuel cell environment.

Acknowledgements

The authors thank MISTRA (The Swedish Foundation for Strategic Environmental Research)/Jungner Centre for financial support, via the programme "Fuel Cells in a Sustainable Society". A.E.C. Palmqvist thanks the Swedish Research Council for a senior researcher grant, and support from the Competence Centre for Catalysis, which is funded by the Swedish Energy Agency and the member companies: AB Volvo, Volvo Car Corporation, Scania CV AB, G.M. Powertrain Sweden AB, Haldor Topsoe A/S, Perstorp Specialty Chemicals AB and The Swedish Space Agency. Gokul Ramamurthy is acknowledged for his preliminary work on the electrochemical evaluation of the Sr_3NiPtO_6 sample.

References

[1] E. Antolini, J. Mater. Sci 38 (2003) 2995–3005.
[2] F.H.B. Lima, E.A. Ticianelli, Electrochim. Acta 49 (2004) 4091–4099.
[3] S. Mukerjee, S. Srinivasan, J. Electroanal. Chem. 357 (1993) 201–224.
[4] U.A. Paulus, A. Wokaun, G.G. Scherer, T.J. Schmidt, V. Stamenkovic, V. Radmilovic, N.M. Markovic, P.N. Ross, J. Phys. Chem. B 106 (2002) 4181–4191.
[5] P. Yu, M. Pemberton, P. Plasse, J. Power Sources 144 (2005) 11–20.
[6] H.R. Colón-Mercado, B.N. Popov, J. Power Sources 155 (2006) 253–263.
[7] G. Faubert, R. Côté, J.P. Dodelet, M. Lefèvre, P. Bertrand, Electrochim. Acta 44 (1999) 2589–2603.
[8] M. Bron, S. Fiechter, P. Bogdanoff, H. Tributsch, Fuel Cells 2 (2003) 137–142.
[9] T. Seiler, E.R. Savinova, K.A. Friedrich, U. Stimming, Electrochim. Acta 49 (2004) 3927–3936.
[10] S.D. Knights, K.M. Colbow, J. St-Pierre, D.P. Wilkinson, J. Power Sources 127 (2004) 127–134.
[11] N. Lempola, B. Steiger, G.G. Scherer, A. Wokaun, Proceedings of the 2nd European PEFC forum 1 (2003) 407–411.
[12] J. Ihonen, F. Jaouen, G. Lindbergh, G. Sundholm, Electrochim. Acta 46 (2001) 2899–2911.
[13] T.N. Nguyen, D.M. Giaquinta, H.-C.z. Loye, Chem. Mater. 6 (1994) 1642–1646.
[14] T.N. Nguyen, H.-C.z. Loye, J. Cryst. Growth 172 (1997) 183–189.
[15] W.H. Henley, J.B. Claridge, P.L. Smallwood, H.-C.z. Loye, J. Cryst. Growth 204 (1999) 122–127.
[16] J.B. Claridge, R.C. Layland, W.H. Henley, H.-C.z. Loye, Chem. Mater. 11 (1999) 1376–1380.
[17] J.M. Bockris, A. Reddy, M. Gamboa-Aldeco, Modern Electrochemistry 2A: Fundamentals of Electrodics, second ed., Kluwer Academic/Plenum Publishers, New York, 2000, pp. 1201–1210.
[18] P.J. Ferreira, G.J.O' l., Y. Shao-Horn, D. Morgan, R. Makharia, S. Kocha, H.A. Gasteiger, J. Electrochem. Soc. 152 (2005) A2256–A2271.